Open Journal of Mathematical Sciences

PSR Press

Article

Thermal analysis of bioconvective gold–silver blood nanofluids in a Sisko fluid with motile microorganisms and radiative effects

Haris Alam Zuberi[1], Roslinda Nazar[2] and Nurul Amira Zainal[3,*]

[1] School of Computational Sciences, Faculty of Science and Technology, JSPM University, Pune, 412207, Maharashtra, India
[2] Fakulti Sains dan Teknologi, Universiti Kebangsaan Malaysia, 43600 UKM Bangi, Selangor, Malaysia
[3] Fakulti Teknologi dan Kejuruteraan Mekanikal, Universiti Teknikal Malaysia Melaka, 76100 Durian Tunggal, Melaka, Malaysia
* Correspondence: nurulamira@utem.edu.my

Received: 23 Dec 2025; Revised: 15 Feb 2026; Accepted: 21 Feb 2026; Published: 10 Apr 2026

Abstract: The increasing relevance of nanofluids in biomedical heat and mass transfer applications has driven the need for more biologically realistic models that can accurately represent the micro-scale dynamics of blood flow. Motivated by this need, this research introduces a novel bio-convective formulation by coupling the effects of nanoparticle-enhanced conductivity with microorganism-induced convection, providing a comprehensive theoretical framework for bioconvective transport of non-Newtonian bio-nanofluids over a nonlinear stretching surface. The model is intended as an idealized representation of shear-driven transport mechanisms relevant to microfluidic and bio-inspired thermal systems. The governing boundary-layer equations for momentum, energy, and microorganism concentration are transformed via similarity variables and solved numerically using the Runge–Kutta–Fehlberg (RKF45) method with the shooting technique. The results reveal that the inclusion of motile microorganisms significantly modifies the flow structure, reducing their accumulation near the surface with increasing nanoparticle concentration, radiation, and magnetic effects. Comparisons between gold and silver-based nanofluids reveal that gold-based suspensions maintain higher thermal energy levels, accompanied by increased viscous resistance and diminished microorganism transport. Parametric analyses indicate that higher nanoparticle concentrations and magnetic field strength lead to reduced velocity and microorganism density, while enhancing the fluid's temperature due to augmented viscous and Joule heating. Furthermore, increasing the nonlinear stretching parameter and Prandtl number improves convective cooling but restricts microorganism transport. While biomedical applications are discussed for motivation, the present configuration does not represent a patient-specific arterial geometry.

Keywords: Sisko model, gold-blood, silver-blood, nanofluid, Runge-Kutta-Fehlberg, motile micro-organisms

MSC: 76A05, 76D10, 65L06.

1. Introduction

Nanofluids, colloidal suspensions of nanoparticles in base fluids, have emerged as an effective medium to enhance heat and mass transfer rates in complex fluid flow systems. In biomedical engineering, the use of biocompatible nanoparticles such as gold and silver has shown tremendous promise due to their unique physical and chemical properties [1]. The modeling of such fluids flowing through stenosed arteries has gained traction, with numerous studies focusing on non-Newtonian behavior, magnetic fields, chemical reactions, and bioconvection. Gold nanoparticles (AuNPs), owing to their high surface area-to-volume ratio, thermal conductivity, and compatibility with human tissues, are frequently employed in medical modeling. For instance, Algehyne et al. [2] conducted an entropy-optimized study involving drug delivery using Au–Ta hybrid nanofluids flowing through stenosed arteries, demonstrating the effectiveness of nanoparticle-mediated thermal therapies. Similarly, Fangfang et al. [3] developed a trihybrid Sisko nanofluid

model to explore the rheological behavior and heat transfer performance in a biomedical flow context, indicating enhanced energy transport due to complex nanofluid interactions.

The Sisko fluid model, a subclass of non-Newtonian fluids, offers flexibility in capturing both shear-thinning and shear-thickening behaviors, making it particularly suitable for simulating blood under various physiological conditions. Waqas et al. [4] investigated Sisko gold nanofluid flow influenced by thermal radiation, magnetic fields, and slip conditions, underscoring the significance of nanoparticle shape factors in optimizing the fluid's thermal performance. Similarly, Eid et al. [5] explored radiation effects in a Sisko-based gold-blood nanofluid model, revealing the enhancement of thermal energy transfer in radiative environments. Eid and Ahmed [6] extended this framework to investigate hybrid nanofluids and presented analytical solutions using the homotopy analysis method, confirming the reliability of semi-analytical techniques in such complex systems. The irreversible nature of energy dissipation, often characterized through entropy generation, is critical in evaluating the efficiency of nanofluid systems. Reddy et al. [7] addressed this by analyzing electrokinetically driven peristaltic flows of nanofluids in microchannels, incorporating entropy generation and nonlinear thermal radiation. Their findings provided insights into microscale fluid manipulation with electro-osmotic influences. Furthermore, Tang et al. [8] incorporated porous walls into Sisko blood flow models in stenotic arteries, revealing additional resistance to flow due to porosity. The same authors [9] also investigated the magnetohydrodynamic (MHD) behavior of Oldroyd-B nanofluids in arterial geometries, suggesting a trade-off between magnetic field strength and thermal efficiency.

Incorporating biological elements, such as motile microorganisms, introduces bioconvective phenomena that further complicate and enrich the transport behavior of nanofluids. Sajid et al. [10] included Brownian motion and species diffusivity in their MHD Sisko nanofluid model with motile microorganisms, highlighting how microbial activity can enhance convective flows. Khan et al. [11] modeled heat and mass transfer in Sisko gold-blood nanofluids under partial slip conditions and MHD, emphasizing the effects of variable thermal conductivity and nanoparticle volume fraction on transport phenomena. The three-dimensional dynamics of radiative bioconvective Sisko flows with microorganisms were explored by Ge-JiLe et al. [12], who introduced microbial activity and radiative parameters to study the convective instabilities and transport enhancement. In a similar vein, Nisar et al. [13] incorporated Joule heating and magnetic fields in Sisko gold nanofluids with thermal radiation effects. Safiullah and De [14] applied artificial neural networks to simulate heat generation and absorption in gold-based Sisko fluids, demonstrating the usefulness of machine learning techniques in modeling nonlinear transport equations.

The concept of entropy generation in nanofluid systems was further advanced by Tao et al. [15], who modeled bioconvective micropolar nanofluids over stretching sheets, accounting for gyrotactic motility and variable fluid properties. Mebarek-Oudina [16] supported this by conducting computational fluid dynamics (CFD) simulations of blood flow involving gold and silver nanoparticles, reinforcing the importance of simulation tools in biomedical flow analysis. Rahman et al. [17] extended the investigation of bioconvective phenomena in Sutterby nanofluids, introducing chemical reactions, activation energy, and nonlinear thermal radiation. These studies revealed how the interaction of biological and physical factors affects heat and mass transport in bio-nanofluid systems. Ali et al. [18] incorporated Darcy-Forchheimer porous media effects and Jeffrey fluid assumptions in their analysis, showing the decelerating influence of porous drag and the enhancing role of thermal conductivity. The inclusion of a magnetic dipole and viscous dissipation was explored by Ijaz et al. [19] in their study of bio-convective flows of Casson nanofluids, while Bibi et al. [20] utilized non-Fourier heat flux models to simulate bio-convective flow of silver-blood nanofluids, emphasizing the distinct role of different nanoparticle materials in biomedical contexts. Tang et al. [21] used advanced sensitivity analysis to study the combined effects of radiation, motility, and magnetic forces in Carreau nanofluids, providing deeper insights into the controllability of such systems. Activation energy and bioconvective instabilities were thoroughly studied by Khan et al. [22], who showed the critical dependence of reaction rates and motility on temperature gradients. Alqarni et al. [23] introduced Marangoni convection into the modeling of Jeffrey nanofluids containing motile microorganisms, revealing surface-tension-driven effects on transport.

Porous wall flows were addressed by Nisha and De [24], who examined variable viscosity and electro-osmotic effects in Sisko fluid systems. Ramasekhar et al. [25] applied the finite element method to model gold and Fe_3O_4 nanoparticle flows in stenosed arteries, yielding results relevant to therapeutic hyperthermia. Further enhancement of nanofluid performance in porous channels was examined by Tang

et al. [8] and Naqvi et al. [26], who investigated stretching surfaces and magnetic field interactions. The role of variable porosity and chemical reactions in blood-based AuNP flow was modeled by Kumar and Benazir [27], while Mandal and Pal [28] focused on entropy generation in gold-silver blood nanofluids flowing through stenotic arteries. Hybrid Casson models were employed by Ramasekhar and Shah [29], and Najafi et al. [30] compared various nanocomposites in pulsatile blood flow, suggesting design strategies for optimal heat transport.

Hafed et al. [31] developed new bio-convective frameworks for radiative flow with motile organisms. Stratification effects in Jeffrey fluids were modeled by Muhammad et al. [32], and Reiner-Rivlin fluid interactions with microorganisms were studied by Khan et al. [33]. Waqas et al. [34] included rotational effects in gold-silver-blood nanofluids over disks, presenting novel geometrical influences on transport properties. Lastly, Nisar and Yasmin [35] studied peristaltic flows with gyrotactic microorganisms under the Carreau–Yasuda model, encapsulating a comprehensive view of nonlinear, bio-inspired nanofluid dynamics.

Despite significant advancements in modeling nanofluid dynamics within biomedical contexts, most existing studies have largely focused on classical heat and mass transfer mechanisms without adequately addressing the biological complexity introduced by motile microorganisms. The inclusion of gyrotactic microorganisms into the nanofluid model introduces a novel dimension of bioconvective behavior, which significantly alters fluid stability, nutrient transport, and thermal performance. This addition not only accounts for the self-propelled motion of microbes but also replicates the natural bioconvection observed in microbial suspensions, a phenomenon critical in optimizing oxygen and nutrient delivery in therapeutic applications. Unlike prior works [4,6,9,19] that primarily examined thermal effects, magnetic fields, or chemical reactions, our study uniquely integrates motile microorganisms within a Sisko gold/silver-blood nanofluid under the influence of thermal radiation and nonlinear heat generation. It is important to emphasize that the present investigation does not aim to model a realistic arterial geometry. Instead, the nonlinear stretching-sheet configuration is adopted as a canonical and mathematically tractable framework to isolate the coupled effects of non-Newtonian rheology, nanoparticle-enhanced thermal transport, magnetic field, and bioconvection induced by motile microorganisms. Such stretching-surface models are widely used in the literature as idealized analogues for shear-driven transport in bio-inspired and microfluidic systems. Any discussion related to blood flow or biomedical relevance is therefore intended to be qualitative and motivational rather than a direct physiological prediction.

2. Constitution of the problem

The physical configuration considered in this study represents an idealized two-dimensional nonlinear stretching surface immersed in a bio-nanofluid. The stretching sheet serves as a simplified boundary to model shear-induced transport phenomena and does not correspond to a physical arterial wall or tubular blood vessel. Consequently, the governing equations and boundary-layer assumptions are formulated for a generic stretching-sheet flow rather than a realistic arterial geometry. The present study investigates the two-dimensional, steady boundary-layer flow of a Sisko nanofluid containing either gold or silver nanoparticles suspended in a blood-based medium. The flow is considered over a non-linear stretching sheet, which drives the fluid motion along the horizontal x-axis, while the vertical y-axis is oriented perpendicular to the surface. The stretching velocity is assumed to vary as a power function of the form $U_w(x) = cx^m$, where c is a positive constant and m is the non-linear stretching parameter. The nanofluid is modeled as incompressible and electrically conducting, subject to the influence of an externally applied transverse magnetic field of constant strength B_0 along the y-direction.

Thermal behavior is incorporated by considering a surface temperature T_w at the wall and an ambient temperature T_∞ at the far field. The effects of thermal radiation are also included in the energy equation to capture radiative heat transfer in the boundary layer accurately. Additionally, the fluid is assumed to contain uniformly distributed motile microorganisms that contribute to bioconvection. Their distribution is governed by a microorganism concentration equation, which accounts for chemotaxis and motility effects. The inclusion of this bio-convective aspect allows for a more comprehensive understanding of transport phenomena in nanofluids for biomedical and microfluidic applications.

Under the boundary layer approximations, the governing equations for conservation of mass, momentum, energy, and motile microorganism concentration are formulated in Cartesian coordinates as follows:

$$u_x + v_y = 0, \tag{1}$$

$$uu_x + vu_y = \frac{a}{\rho_{nf}} u_{yy} - \frac{b}{\rho_{nf}} \frac{\partial}{\partial y} (u_y)^n - \frac{\sigma_{nf} B_0^2}{\rho_{nf}} u, \tag{2}$$

$$uT_x + vT_y = \alpha_{nf} T_{yy} - \frac{1}{(\rho c_p)_{nf}} \frac{\partial}{\partial y} (q_r), \tag{3}$$

$$uN_x + vN_y = D_m N_{yy} - W_c N_y, \tag{4}$$

with boundary conditions

$$\begin{aligned} &u = u_w = cx^m, \quad v = 0, \quad T = T_w, \quad N = N_w \quad \text{at } y = 0, \\ &u \to 0, \quad T \to T_\infty, \quad N \to N_\infty \quad \text{as } y \to \infty. \end{aligned} \tag{5}$$

These equations are then transformed using similarity variables to reduce the partial differential equations into a system of coupled non-linear ordinary differential equations. The resulting system captures the essential physical behavior of the nanofluid in the presence of a magnetic field, thermal radiation, and a non-linear stretching surface, while also considering the transport of motile microorganisms within the boundary layer. This formulation serves as the foundation for the numerical investigation presented in the subsequent sections.

Velocity of nanofluid is $(x, y, 0)$, a, b, and n are the constants of material for Sisko bio-nanofluid. T is the nanofluid temperature, ρ_{nf} is the nanofluid's density, nanofluid's thermal diffusivity is given by

$$\alpha_{nf} = \frac{k_{nf}}{(\rho c_p)_{nf}},$$

c_p is the specific heat at constant pressure, and k_{nf} is the nanofluid's thermal conductivity, which are described as:

$$\left.\begin{aligned} \rho_{nf} &= (1-\varphi)\rho_b + \varphi\rho_g, \\ (\rho c_p)_{nf} &= (1-\varphi)(\rho c_p)_b + \varphi(\rho c_p)_g, \\ k_{nf}^{(Au)} &= k_b \frac{(k_{Au} + 2k_b) - 2\varphi(k_b - k_{Au})}{(k_{Au} + 2k_b) + \varphi(k_b - k_{Au})}, \\ k_{nf}^{(Ag)} &= k_b \frac{(k_{Ag} + 2k_b) - 2\varphi(k_b - k_{Ag})}{(k_{Ag} + 2k_b) + \varphi(k_b - k_{Ag})}, \end{aligned}\right\} \tag{6}$$

where φ represents the volume fraction of nanoparticles, ρ_b denotes the density of blood and ρ_g denotes the density of the nanoparticles. The terms $(\rho c_p)_b$ and $(\rho c_p)_g$ represent the heat capacitances of blood and nanoparticles, respectively, while k_b, k_{Au}, and k_{Ag} denote the thermal conductivities of blood, gold and silver nanoparticles. The radiative heat flux q_r is given by

$$q_r = -\frac{4\sigma^*}{3k^*} \frac{\partial T^4}{\partial y}, \tag{7}$$

where σ^* and k^* are the Stefan–Boltzmann constant and the coefficient of mean absorption, respectively. Expanding T^4 in powers of T using the Taylor series and neglecting higher-order terms, the following approximation is obtained:

$$T^4 \approx 4T_\infty^3 T - 3T_\infty^4. \tag{8}$$

Introducing the following non-dimensionalizing functions,

$$\left.\begin{aligned} \eta &= \frac{y}{x}\,\mathrm{Re}_b^{\frac{1}{n+1}}, \\ u &= u_w f'(\eta), \\ v &= -u_w \mathrm{Re}_b^{\frac{1}{n+1}} \left\{[m(2n-1)+1]f(\eta) + [m(2-n)-1]\eta f'(\eta)\right\}, \\ \theta &= \frac{T-T_\infty}{T_w-T_\infty}, \\ \chi &= \frac{N-N_\infty}{N_w-N_\infty}. \end{aligned}\right\} \tag{9}$$

The transformed equations take the form

$$Af''' + n(f'')^{n-1}f''' + \left[(1-\varphi) + \varphi\frac{\rho_g}{\rho_b}\right]\left[\frac{m(2n-1)+1}{n+1}ff'' - m(f')^2\right] - Mf' = 0, \tag{10}$$

$$\frac{1}{\mathrm{Pr}}\left(1+\frac{4}{3R_d}\right)\left(\frac{k_{nf}}{k_b}\right)\theta'' + \frac{m(2n-1)+1}{n+1}\left[(1-\varphi) + \varphi\frac{(\rho c_p)_g}{(\rho c_p)_b}\right]f\theta' = 0, \tag{11}$$

$$\chi'' + \mathrm{Le}\left[f\chi' - \beta\chi\right] = 0, \tag{12}$$

and the boundary conditions become

$$\begin{cases} f(0)=0, \quad f'(0)=1, \quad \theta(0)=1, \quad \chi(0)=1, \\ f'(\infty)\to 0, \quad \theta(\infty)\to 0, \quad \chi(\infty)\to 0, \end{cases} \tag{13}$$

where

$$\left.\begin{aligned} A &= \frac{\mathrm{Re}_b^{\frac{2}{n+1}}}{\mathrm{Re}_a}, \quad \mathrm{Pr} = \frac{xu_w}{\alpha_b}\,\mathrm{Re}_b^{-\frac{2}{n+1}}, \quad M = \frac{\sigma_{nf}B_0^2 x}{\rho_{nf}u_w}, \\ \mathrm{Re}_a &= \frac{\rho_b x u_w}{a}, \quad \mathrm{Re}_b = \frac{\rho_b x^n u_w^{2-n}}{b}, \quad \alpha_b = \frac{k_b}{(\rho c_p)_b}, \end{aligned}\right\} \tag{14}$$

$$\mathrm{Le} = \frac{\nu}{D_m}, \quad \beta = \frac{W_c}{cx^m}.$$

Here, A is referred to as the Sisko nanofluid material parameter, Pr denotes the Prandtl number, and M represents the magnetic parameter. The quantities Re_a and Re_b are termed the local Reynolds numbers, while α_b denotes the thermal diffusivity of blood. Furthermore, Le represents the Lewis number, D_m is the diffusivity of motile microorganisms, β is the swimming speed parameter, and W_c denotes the average swimming speed of microorganisms. The engineered local Nusselt number and the skin friction coefficient are expressed as:

$$\mathrm{Nu}_x = -\frac{xq_w}{k_b(T_w-T_\infty)}, \quad C_{f_x} = \frac{\tau_w}{\frac{1}{2}\rho_b u_w^2}, \tag{15}$$

where the wall shear stress τ_w and the wall heat flux q_w are defined as

$$\tau_w = \left[a\left(\frac{\partial u}{\partial y}\right) + b\left(\frac{\partial u}{\partial y}\right)^n\right]_{y=0}, \quad q_w = -k_{hnf}\left.\frac{\partial T}{\partial y}\right|_{y=0}. \tag{16}$$

3. Method of solution

The governing equations describing the flow, heat transfer, and motile microorganism transport in a non-Newtonian Sisko nanofluid are highly non-linear and coupled in nature. These equations, derived using appropriate similarity transformations, are initially expressed in terms of higher-order ordinary differential equations (ODEs). In order to facilitate numerical computation, the coupled system is first reduced to a

set of first-order ODEs. This transformation is essential for implementing standard numerical integration techniques and provides a structured framework for efficiently handling the complex interactions among velocity, temperature, and concentration fields.

To obtain accurate and stable solutions, the fourth–fifth order Runge–Kutta–Fehlberg method (RKF45) is employed in conjunction with the shooting technique. The RKF45 method is a widely used adaptive step-size integration scheme that dynamically adjusts the step size based on local error estimates, allowing it to maintain high accuracy while optimizing computational efficiency. Its dual-order formulation (fourth and fifth order) ensures that the integration is robust and reliable, especially for stiff or sensitive systems, as often encountered in non-Newtonian fluid models. The shooting method is used to convert the boundary value problem (BVP) into an equivalent initial value problem (IVP), enabling the RKF45 integrator to propagate solutions from the boundary conditions at the wall ($\eta = 0$) to the far-field ($\eta \to \infty$). Unknown initial conditions are iteratively adjusted using MATLAB's built-in fsolve function until the far-field boundary conditions are satisfied within a prescribed tolerance. In this study, a relative tolerance of 1.0×10^{-6} is adopted to ensure convergence and precision in the computed results. The numerical scheme is implemented in the MATLAB environment, which provides a flexible platform for handling the system of equations, evaluating the adaptive steps, and visualizing the resulting profiles. This method offers several advantages: it avoids the complexities associated with linearization, preserves the nonlinearity of the model, and ensures smooth, continuous solutions for velocity, temperature, and microorganism concentration. The algorithm is capable of handling a wide range of parameter variations without compromising stability, making it particularly effective for the present bio-convective, magnetothermal flow problem

The required thermophysical properties of blood, gold, and silver nanoparticles used in this analysis are presented in Table 1, and serve as the basis for computing the effective dynamic and thermal behavior of the nanofluids. This methodological approach lays the foundation for a reliable parametric investigation, the results of which are comprehensively discussed in the following section

Table 1. Thermo-physical properties for blood, gold (Au) and silver (Ag) nanoparticles

Property	Blood	Au nanoparticles	Ag nanoparticles
ρ (kg/m^3)	1063	19300	10600
C_p (J/kg K)	3594	129.1	235
k (W/m K)	0.492	318	419

4. Numerical results and discussion

The present section focuses on the analysis of the numerical results obtained for the flow, heat transfer, and motile microorganism characteristics of gold-blood and silver-blood nanofluids modeled using the Sisko fluid framework. The system of non-linear ordinary differential equations, derived from the governing partial differential equations through similarity transformations, has been solved numerically using the Runge–Kutta–Fehlberg (RKF45) method combined with a shooting technique. This approach enables the accurate computation of velocity, temperature, and microorganism concentration profiles under the influence of various physical parameters. A comprehensive set of graphs has been generated and explored in Figures 1 to 19 to interpret the influence of these parameters on the behavior of the nanofluid system. Specifically, Figures 1 to 3 present the impact of key parameters on the velocity profiles, Figures 4 to 9 demonstrate their effect on temperature distribution, and Figures 10 to 15 highlight the response of motile microorganism concentration to different physical inputs.

4.1. Velocity profiles

Figure 1 illustrates the velocity profiles for gold-blood and silver-blood nanofluids at various nanoparticle concentrations. It is observed that the velocity decreases with an increase in nanoparticle concentration for both types of nanofluids. This behavior is physically consistent with the modeled Sisko fluid dynamics, where the addition of nanoparticles increases the effective viscosity of the suspension. The elevated viscosity enhances internal resistance within the fluid, thereby reducing the momentum transfer from the stretching surface. As a result, the momentum boundary layer becomes thinner, and the flow velocity diminishes. Furthermore, it

is observed that the gold-blood nanofluid exhibits a lower velocity compared to the silver-blood nanofluid under the same conditions. This is attributed to the higher density and greater viscosity-inducing effect of gold nanoparticles, which intensify the flow resistance and further suppress the velocity profile.

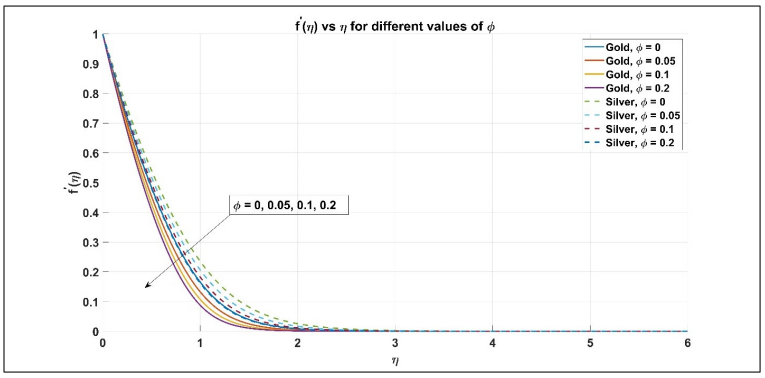

Figure 1. Velocity of gold-blood and silver-blood nanofluids for different values of volume fraction of nanoparticles

Figure 2 presents the velocity profiles of gold- and silver-blood nanofluids for different values of the Sisko material parameter A. It is observed that increasing A significantly alters the velocity distribution within the boundary layer for both nanofluids. Specifically, higher values of A enhance the velocity magnitude near the surface, indicating a reduction in effective resistance to flow associated with the Sisko fluid rheology. This behavior reflects the strong influence of the material parameter A on the non-Newtonian characteristics of the fluid, where variations in shear-dependent viscosity modify the momentum transport mechanism. Furthermore, under identical parameter values, the silver-blood nanofluid exhibits slightly higher velocity profiles compared to the gold-blood nanofluid. This difference can be attributed to the relatively higher viscous resistance induced by gold nanoparticles, which suppresses fluid motion and leads to a thicker momentum boundary layer in the Au-based nanofluid.

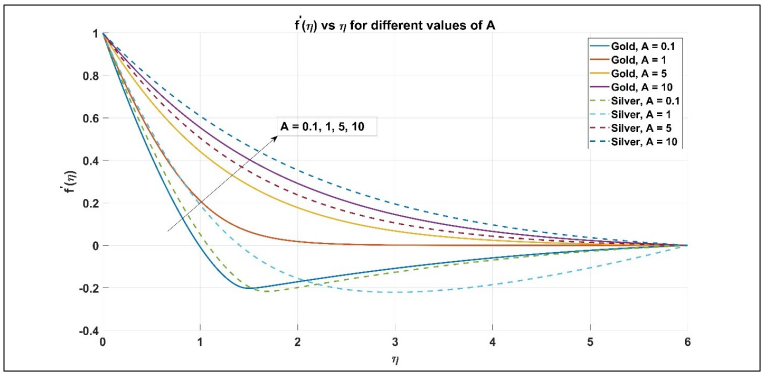

Figure 2. Velocity profiles $f'(\eta)$ versus similarity variable η for gold- and silver-blood nanofluids at different values of the Sisko material parameter

Figure 3 illustrates the velocity profiles of gold-blood and silver-blood nanofluids corresponding to different values of the non-linear stretching parameter. With an increase in the stretching parameter, the velocity of both nanofluids rises. This occurs because a stronger stretching of the surface enhances the shear force applied to the fluid, promoting greater momentum transfer from the boundary. As a result, the flow accelerates and the velocity boundary layer becomes thicker. The figure also indicates that, at each value of the stretching parameter, the gold-blood nanofluid exhibits a slightly lower velocity compared to the silver-blood nanofluid. This difference is due to the higher density and more pronounced viscous effects associated with gold nanoparticles, which contribute to increased resistance against fluid motion.

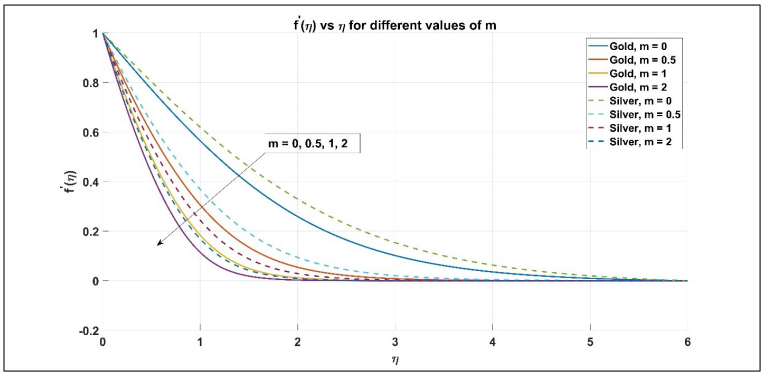

Figure 3. Velocity profiles $f'(\eta)$ versus similarity variable η for gold- and silver-blood nanofluids at different values of the non-linear stretching parameter

4.2. Temperature profiles

Figure 4 displays the temperature profiles of gold-blood and silver-blood nanofluids for different values of nanoparticle concentration. As the concentration increases, the temperature within the boundary layer also rises for both nanofluids. This trend is attributed to the enhanced thermal conductivity introduced by the nanoparticles, which improves the heat transfer capacity of the fluid. With more nanoparticles dispersed in the base fluid, the nanofluid absorbs and retains more thermal energy, resulting in a higher temperature distribution. The gold-blood nanofluid consistently exhibits a higher temperature profile than the silver-blood nanofluid at each concentration level, which can be attributed to enhanced thermal energy retention resulting from increased viscous resistance and reduced convective cooling in the Au-based nanofluid. This allows the gold-based suspension to store and distribute heat more efficiently throughout the fluid domain.

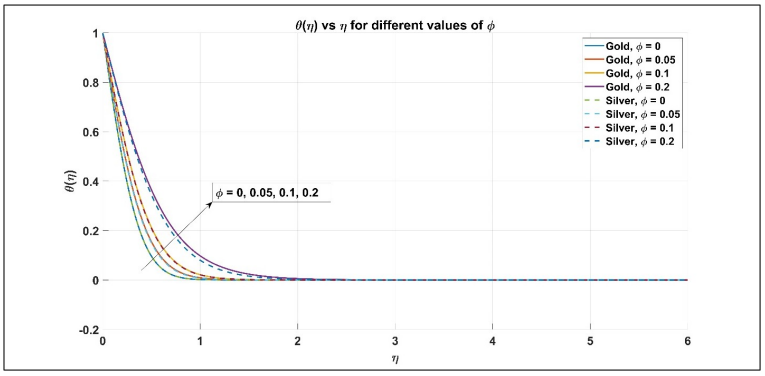

Figure 4. Temperature profiles $\theta(\eta)$ versus similarity variable η of gold-blood and silver-blood nanofluids for different values of volume fraction of nanoparticles

Figure 5 shows the temperature profiles of gold-blood and silver-blood nanofluids for varying values of the Sisko material parameter. As the Sisko parameter increases, the temperature within the boundary layer also increases for both types of nanofluids. This parameter characterizes the non-Newtonian nature of the fluid, where higher values indicate stronger shear-thinning behavior. In the context of the modeled problem, an increase in this parameter reduces the resistance to deformation under shear, resulting in a less effective convective cooling mechanism. Consequently, more thermal energy is retained within the fluid, leading to a rise in temperature. Furthermore, the temperature profile of the gold-blood nanofluid remains consistently higher than that of the silver-blood nanofluid at all values of the Sisko parameter. This is attributed to the enhanced thermal energy retention and suppressed convective transport, which enhances the fluid's ability to absorb and retain heat within the thermal boundary layer.

Figure 6 presents the temperature profiles of gold-blood and silver-blood nanofluids for different values of the non-linear stretching parameter. As the stretching parameter increases, the temperature within the boundary layer decreases for both nanofluids. This occurs because stronger stretching enhances the fluid motion along the surface, which in turn increases convective heat transfer away from the heated surface. As

a result, the thermal boundary layer becomes thinner, and the fluid retains less thermal energy near the wall. The figure also shows that the temperature profile of the gold-blood nanofluid remains higher than that of the silver-blood nanofluid across all stretching rates. This is due to enhanced thermal energy retention and suppressed convective transport, which improves the nanofluid's capacity to absorb and store heat, leading to a warmer thermal boundary layer compared to its silver-based counterpart.

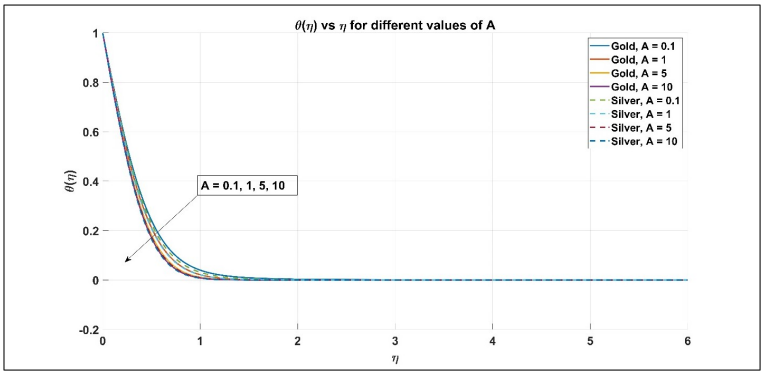

Figure 5. Temperature profiles $\theta(\eta)$ versus similarity variable η of gold-blood and silver-blood nanofluids for different values of Sisko material parameter

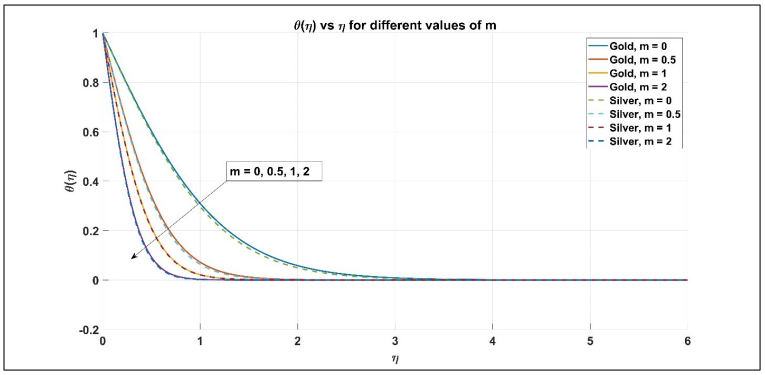

Figure 6. Temperature profiles $\theta(\eta)$ versus similarity variable η of gold-blood and silver-blood nanofluids for different values of non-linear stretching parameter

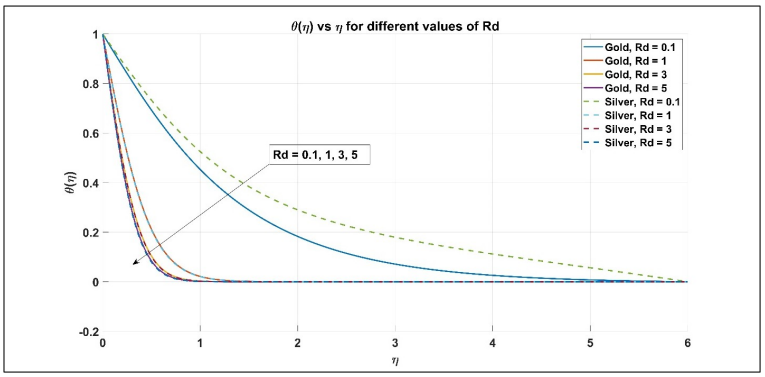

Figure 7. Temperature profiles $\theta(\eta)$ versus similarity variable η of gold-blood and silver-blood nanofluids for different values of magnetic parameter

Figure 7 shows the temperature profiles of gold-blood and silver-blood nanofluids for varying values of the thermal radiation parameter. As the radiation parameter increases, the temperature within the boundary layer also increases. This is because thermal radiation enhances the thermal energy input into the system, leading to a greater accumulation of heat in the fluid. The radiation effect weakens the cooling

efficiency, resulting in a thicker thermal boundary layer. Additionally, the gold-blood nanofluid consistently maintains a higher temperature than the silver-blood nanofluid, which can be attributed to increased thermal energy retention associated with reduced convective cooling and stronger viscous resistance in the Au-based nanofluid under radiative conditions.

Figure 8 displays the temperature profiles of gold-blood and silver-blood nanofluids for different values of the magnetic parameter. An increase in the magnetic parameter leads to a rise in the fluid temperature. This is attributed to the presence of a transverse magnetic field that induces a Lorentz force, which resists fluid motion and generates internal heating known as Joule heating. This internal energy dissipation raises the temperature of the fluid. The temperature profile for the gold-blood nanofluid remains higher than that of the silver-blood nanofluid at each magnetic field strength due to the enhanced thermal storage capability of gold-based nanofluids.

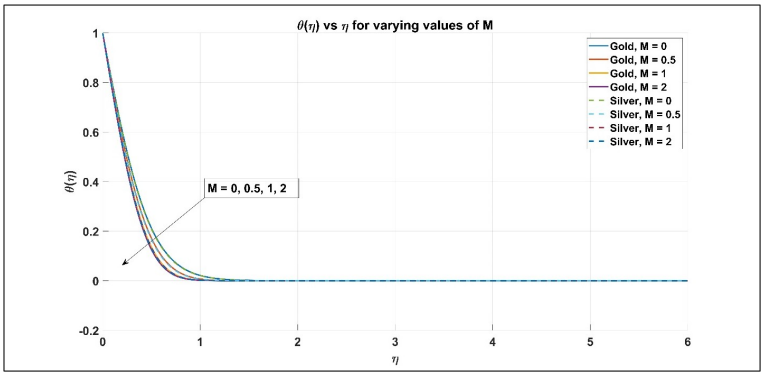

Figure 8. Temperature profiles $\theta(\eta)$ versus similarity variable η of gold-blood and silver-blood nanofluids for different values of magnetic parameter

Figure 9 illustrates the temperature profiles of gold-blood and silver-blood nanofluids for varying values of the Prandtl number. As the Prandtl number increases, the fluid temperature decreases. This is because a higher Prandtl number signifies lower thermal diffusivity, which means the fluid transfers heat more slowly, leading to a thinner thermal boundary layer and lower temperature distribution. Between the two, the gold-blood nanofluid exhibits a higher temperature profile than the silver-blood nanofluid for all Prandtl number values, primarily due to the greater thermal conductivity of gold nanoparticles, which enhances heat retention within the fluid.

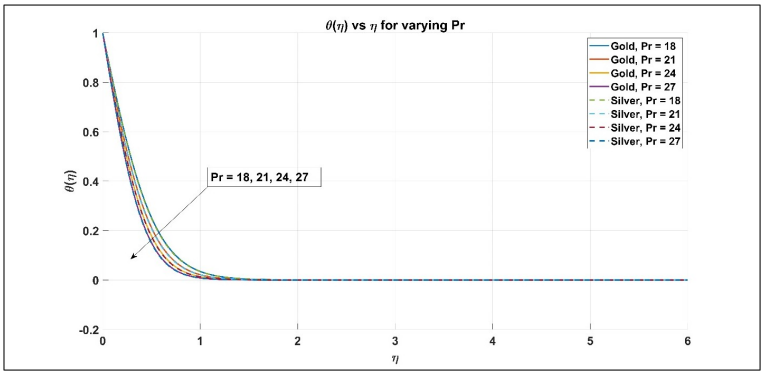

Figure 9. Temperature profiles $\theta(\eta)$ versus similarity variable η of gold-blood and silver-blood nanofluids for different values of Prandtl number

4.3. Motile organisms' concentration profiles

Figure 10 illustrates the concentration profiles of motile microorganisms in gold-blood and silver-blood nanofluids for different values of nanoparticle concentration. As the concentration of nanoparticles increases, the concentration of motile microorganisms decreases throughout the boundary layer. This behavior is attributed to the rise in effective viscosity and thermal conductivity of the nanofluid, both of which alter the

fluid environment in a way that suppresses the motility and dispersion of microorganisms. The enhanced viscosity introduces greater resistance to microorganism movement, while increased thermal conductivity affects the local temperature gradients that often guide microorganism navigation. Additionally, the gold-blood nanofluid exhibits a lower microorganism concentration compared to the silver-blood nanofluid at each level of nanoparticle concentration. This is due to the stronger thermal and viscous effects associated with gold nanoparticles, which more effectively hinder the transport and accumulation of motile microorganisms within the flow field.

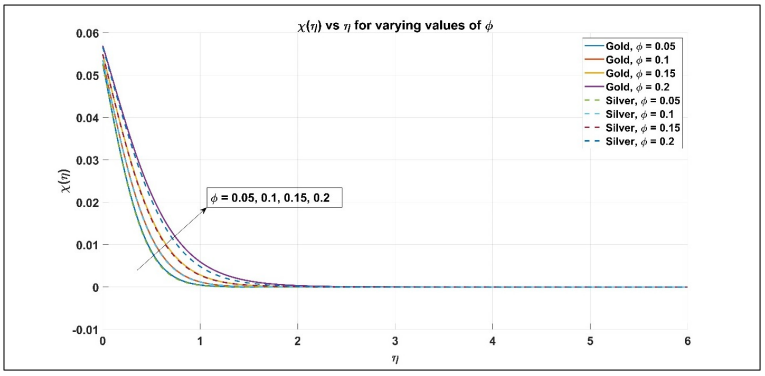

Figure 10. Concentration of motile micro-organisms for different values of volume fraction of nanoparticles

Figure 11 presents the concentration profiles of motile microorganisms in gold-blood and silver-blood nanofluids for varying values of the Sisko material parameter. As this parameter increases, the concentration of motile microorganisms decreases. A higher Sisko parameter reflects stronger shear-thinning behavior, which reduces viscous resistance and accelerates fluid motion. This enhanced flow diminishes the time microorganisms spend near the surface, weakening their accumulation within the boundary layer. The gold-blood nanofluid consistently shows a lower microorganism concentration compared to silver-blood, due to the stronger viscous and thermal interactions introduced by gold nanoparticles, which further hinder microorganism motility.

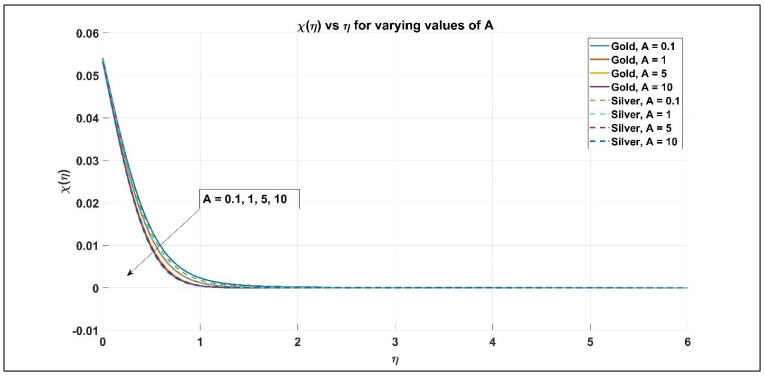

Figure 11. Concentration of motile micro-organisms for different values of Sisko material parameter

Figure 12 shows the concentration of motile microorganisms for different values of the non-linear stretching parameter. With increasing stretching intensity, a noticeable reduction in microorganism concentration is observed. This occurs because stronger stretching accelerates the fluid near the wall, thinning the concentration boundary layer and reducing the opportunity for microorganisms to cluster. The gold-blood nanofluid exhibits a comparatively lower concentration of microorganisms across all stretching values, which is linked to the higher resistance effects induced by gold nanoparticles.

Figure 13 depicts the concentration profiles of motile microorganisms for various values of the thermal radiation parameter. An increase in radiation results in a decline in microorganism concentration for both nanofluids. Enhanced thermal radiation elevates the fluid temperature and disrupts the temperature gradients that typically support microorganism transport via thermotaxis. This weakens their directed movement and

reduces their presence near the surface. The gold-blood nanofluid again shows lower concentration levels, influenced by its greater ability to absorb and distribute radiative heat, which intensifies these effects.

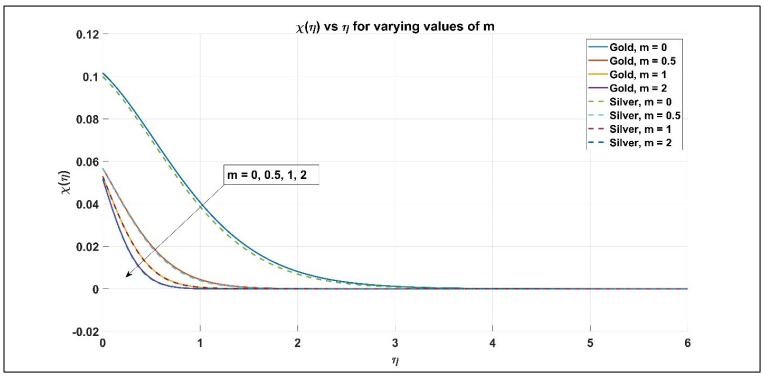

Figure 12. Concentration of motile micro-organisms for different values of non-linear stretching parameter

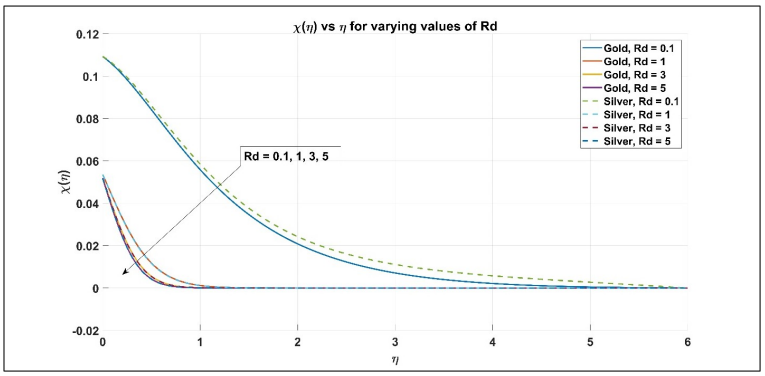

Figure 13. Concentration of motile micro-organisms for different values of thermal radiation parameter

Figure 14 presents the microorganism concentration for different values of the swimming speed parameter. As the swimming speed increases, the concentration of motile microorganisms also increases. This is because higher swimming speed enhances the ability of microorganisms to overcome fluid resistance and remain closer to the surface, promoting accumulation in the boundary layer. However, the concentration in gold-blood nanofluid remains slightly lower than in silver-blood due to stronger viscous and thermal effects in the former, which still impose some restriction on microorganism motility.

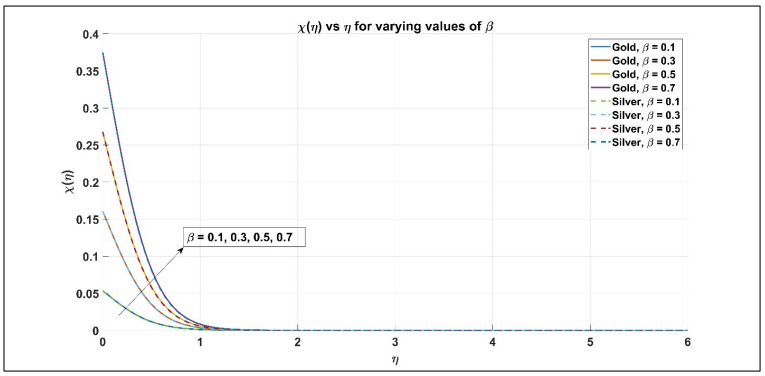

Figure 14. Concentration of motile micro-organisms for different values of the swimming speed parameter b

Figure 15 shows the concentration profiles of motile microorganisms for varying values of the Lewis number. With an increase in the Lewis number, the microorganism concentration decreases. A higher Lewis number indicates reduced mass diffusivity relative to thermal diffusivity, which weakens the transport of microorganisms across the fluid domain. As a result, their distribution becomes more confined and less

pronounced. The gold-blood nanofluid exhibits a lower concentration in comparison to silver-blood at all Lewis number values, due to its enhanced thermal properties and greater suppression of mass transport mechanisms.

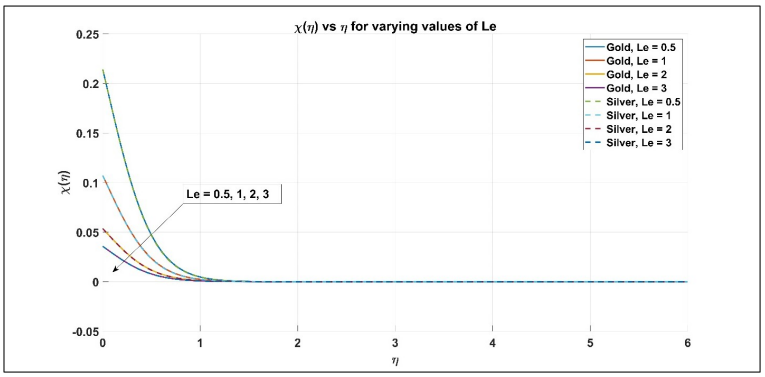

Figure 15. Concentration of motile micro-organisms for different values of Lewis number *Le*

In summary, beyond the qualitative profile analysis, the numerical results also demonstrate clear quantitative trends in key engineering performance measures. An increase in the magnetic parameter leads to higher skin-friction coefficients, indicating enhanced flow resistance, while simultaneously increasing the local Nusselt number due to suppressed convective heat transport and greater thermal energy retention. Thermal radiation exhibits a stronger influence on heat transfer than on momentum transport, whereas variations in the Prandtl number primarily affect the thermal response with comparatively weaker impact on velocity. Comparisons between Au- and Ag-based nanofluids reveal that gold-based nanofluids generally exhibit higher surface shear and enhanced heat transfer rates under identical conditions, reflecting a trade-off between thermal enhancement and increased flow resistance. Among the parameters examined, nanoparticle volume fraction and thermal radiation show the strongest sensitivity in thermal performance, while the influence of magnetic effects on microorganism transport remains comparatively weak.

5. Conclusion

In this study, a computational investigation was carried out to analyze the flow, thermal, and bioconvective characteristics of gold-blood and silver-blood nanofluids under the influence of thermal radiation, magnetic field, and nonlinear stretching. The governing boundary layer equations for momentum, energy, and motile microorganism concentration were formulated using the Sisko non-Newtonian fluid model. These equations were transformed into a system of ordinary differential equations using similarity transformations and solved numerically by employing the Runge–Kutta–Fehlberg (RKF45) method with a shooting technique in MATLAB. The effects of key physical parameters such as nanoparticle concentration, Sisko material parameter, magnetic field, radiation, Prandtl number, and swimming speed on velocity, temperature, and microorganism profiles were investigated in detail for both gold and silver nanoparticles suspended in blood. From the simulation results, the following major conclusions can be drawn:

- Increasing the concentration of nanoparticles leads to a reduction in velocity and motile microorganism concentration, while significantly enhancing the temperature profile due to improved thermal conductivity.
- A higher Sisko material parameter boosts both velocity and temperature, while reducing the concentration of microorganisms, owing to its shear-thinning nature.
- The nonlinear stretching parameter enhances fluid velocity and reduces both temperature and microorganism concentration by intensifying shear near the wall.
- Thermal radiation elevates the temperature while simultaneously reducing microorganism concentration due to disrupted thermotaxis.
- The application of a magnetic field increases fluid temperature as a result of Joule heating, while slowing down the velocity due to Lorentz force resistance.
- A higher Prandtl number reduces the temperature distribution by limiting thermal diffusivity, with gold-blood nanofluids consistently retaining more heat than silver-based ones.

- An increase in the swimming speed of microorganisms promotes their accumulation, whereas higher Lewis numbers suppress their concentration by reducing mass diffusivity.

Overall, the study confirms that gold nanoparticles are more effective than silver in enhancing thermal behavior, although they introduce greater viscous resistance to flow and microorganism motility. These findings offer qualitative insights into the thermal and bioconvective characteristics of bio-nanofluid systems under shear-driven transport conditions.

Author Contributions: Haris Alam Zuberi contributed to the study design and data analysis. Roslinda Nazar contributed to theoretical development and critical revision of the manuscript. Nurul Amira Zainal drafted and revised the manuscript and coordinated the work. All authors approved the final version and agree to be accountable for all aspects of the research.

Conflicts of Interest: No potential competing interest was reported by the author(s).

Acknowledgments: This research is supported Ministry of Higher Education (MoHE) Malaysia, grant number FRGS/1/2024/STG06/UTEM/03/1. The authors would also like to acknowledge Universiti Teknikal Malaysia Melaka for the encouragement in conducting this research.

References

[1] Raju, C. S. K., Basha, H. T., Noor, N. F. M., Shah, N. A., & Yook, S. J. (2024). Significance of body acceleration and gold nanoparticles through blood flow in an uneven/composite inclined stenosis artery: A finite difference computation. *Mathematics and Computers in Simulation, 215*, 399-419.

[2] Algehyne, E. A., Ahammad, N. A., Elnair, M. E., Zidan, M., Alhusayni, Y. Y., El-Bashir, B. O., ... & Alzahrani, F. (2023). Entropy optimization and response surface methodology of blood hybrid nanofluid flow through composite stenosis artery with magnetized nanoparticles (Au-Ta) for drug delivery application. *Scientific Reports, 13*(1), 9856.

[3] Fangfang, F., Sajid, T., Jamshed, W., Eid, M. R., Altamirano, G. C., Altaf, I., ... & El Din, S. M. (2023). Thermal transport and characterized flow of trihybridity Tiwari and Das Sisko nanofluid via a stenosis artery: a case study. *Case Studies in Thermal Engineering, 47*, 103064.

[4] Waqas, H., Farooq, U., Muhammad, T., & Manzoor, U. (2022). Importance of shape factor in Sisko nanofluid flow considering gold nanoparticles. *Alexandria Engineering Journal, 61*(5), 3665-3672.

[5] Eid, M. R., Alsaedi, A., Muhammad, T., & Hayat, T. (2017). Comprehensive analysis of heat transfer of gold-blood nanofluid (Sisko-model) with thermal radiation. *Results in Physics, 7*, 4388-4393.

[6] Eid, M. R., & Al-Hossainy, A. F. (2023). Combined experimental thin film, DFT-TDDFT computational study, flow and heat transfer in [PG-MoS2/ZrO2] C hybrid nanofluid. *Waves in Random and Complex Media, 33*(1), 1-26.

[7] Reddy, S. R. R., Basha, H. T., & Duraisamy, P. (2022). Entropy generation for peristaltic flow of gold-blood nanofluid driven by electrokinetic force in a microchannel. *The European Physical Journal Special Topics, 231*(11), 2409-2423.

[8] Tang, T. Q., Rooman, M., Vrinceanu, N., Shah, Z., & Alshehri, A. (2022). Blood flow of Au-nanofluid using Sisko model in stenotic artery with porous walls and viscous dissipation effect. *Micromachines, 13*(8), 1303.

[9] Tang, T. Q., Rooman, M., Shah, Z., Jan, M. A., Vrinceanu, N., & Racheriu, M. (2023). Computational study and characteristics of magnetized gold-blood Oldroyd-B nanofluid flow and heat transfer in stenosis narrow arteries. *Journal of Magnetism and Magnetic Materials, 569*, 170448.

[10] Sajid, T., Tanveer, S., Munsab, M., & Sabir, Z. (2021). Impact of oxytactic microorganisms and variable species diffusivity on blood-gold Reiner–Philippoff nanofluid. *Applied Nanoscience, 11*(1), 321-333.

[11] Khan, U., Zaib, A., & Ishak, A. (2021). Magnetic field effect on Sisko fluid flow containing gold nanoparticles through a porous curved surface in the presence of radiation and partial slip. *Mathematics, 9*(9), 921.

[12] Ge-JiLe, H., Waqas, H., Khan, S. U., Khan, M. I., Farooq, S., & Hussain, S. (2021). Three-dimensional radiative bioconvective flow of a sisko nanofluid with motile microorganisms. *Coatings, 11*(3), 335.

[13] Nisar, Z., Ahmed, B., Ghazwani, H. A., Muhammad, K., Hussien, M., & Aziz, A. (2023). Numerical study for bioconvection peristaltic flow of Sisko nanofluid with Joule heating and thermal radiation. *Heliyon, 9*(12), e14590.

[14] Safiullah, S. N., & De, P. (2026). Thermal radiation, heat generation/absorption effect on bioconvective Sisko nanofluids over Darcy Forchheimer porous medium with regression analysis. *Numerical Heat Transfer, Part B: Fundamentals, 87*(1), 2390099.

[15] Tao, S. J., Haq, F., Hussain, A., Shokri, A., Ali, M. R., & Hendy, A. S. (2024). Computational framework for thermal transportation in radiative bio-convective micropolar nanomaterial flow over stretched sheet with entropy optimization. *Case Studies in Thermal Engineering, 59*, 104549.

[16] Mebarek-Oudina, F. (Ed.). (2025). CFD simulation: *Thermo-Fluids and Nanofluids in Engineering and Biomedicine* (Vol. 10). Walter de Gruyter GmbH & Co KG.

[17] Rahman, M. U., Haq, F., Ghazwani, H. A., Ghazwani, M. H., & Alnujaie, A. (2024). Heat transport and entropy generation in bioconvective sutterby nanofluid flow with gyrotactic microorganisms and chemical reaction. *Journal of Thermal Analysis and Calorimetry, 149*(23), 14289-14302.

[18] Ali, M. H., Abbas, S. T., Sohail, M., & Singh, A. (2024). Study of bioconvection phenomenon in Jefferey model in a Darcy-Forchheimer porous medium. *BioNanoScience, 14*(4), 4666-4678.

[19] Ijaz, M., Nadeem, S., Ayub, M., & Mansoor, S. (2021). Simulation of magnetic dipole on gyrotactic ferromagnetic fluid flow with nonlinear thermal radiation: M. Ijaz et al. *Journal of Thermal Analysis and Calorimetry, 143*(3), 2053-2067.

[20] Bibi, T., Sagheer, M., & Shahzad, H. (2025). A theoretical study on (TiO 2+ Ag)/EO hybrid Casson nanofluid with motile micro-organisms in non-Fourier heat flux model. *Multiscale and Multidisciplinary Modeling, Experiments and Design, 8*(4), 209.

[21] Tang, T. Q., Shah, Z., Thumma, T., Rooman, M., Vrinceanu, N., & Alshehri, M. H. (2023). Response surface optimization and sensitive analysis on biomagnetic blood Carreau nanofluid flow in stenotic artery with motile gyrotactic microorganisms. *SN Applied Sciences, 5*(12), 355.

[22] Khan, S. U., Al-Khaled, K., Aldabesh, A., Awais, M., & Tlili, I. (2021). Bioconvection flow in accelerated couple stress nanoparticles with activation energy: bio-fuel applications. *Scientific Reports, 11*(1), 3331.

[23] Alqarni, M. S., Waqas, H., Manzoor, U., & Muhammad, T. (2025). Marangoni transport of Jeffrey nanofluid due to circular horizontal cylinder with motile microorganisms. *Waves in Random and Complex Media, 35*(3), 5062-5081.

[24] Nisha, S. S., & De, P. (2024). Impact of electro-osmotic, activation energy and chemical reaction on Sisko fluid over Darcy–Forchheimer porous stretching cylinder. *Proceedings of the Institution of Mechanical Engineers, Part E: Journal of Process Mechanical Engineering*, 09544089241255657.

[25] Ramasekhar, G., Shaik, J., Reddisekhar Reddy, S. R., Divya, A., Jawad, M., & Ali Yousif, B. A. (2026). Numerical investigation of Casson fluid flow performance of blood containing gold and Fe3O4 nanofluid injected into a stenotic artery. *Numerical Heat Transfer, Part A: Applications, 87*(1), 2372465.

[26] Naqvi, S. M. R. S., Farooq, U., Aiyashi, M. A., & Waqas, H. (2022). Comprehensive analysis of thermally radiative transport of Sisko fluid over a porous stretchable curved surface with gold nanoparticles. *International Journal of Modern Physics B, 36*(03), 2250028.

[27] Kumar, C. M., & Benazir, A. J. (2026). Bioconvective flow of blood suspended with AuNPs over a stretching sheet with variable porosity and permeability. *Numerical Heat Transfer, Part A: Applications, 87*(1), 2389337.

[28] Mandal, G., & Pal, D. (2024). Impact of gold and silver nanoparticles on the thermally radiating MHD slip blood flow within the stenotic artery using stability analysis and entropy optimisation. *Pramana, 98*(4), 157.

[29] Ramasekhar, G., & Shah, N. A. (2025). Theoretical investigation of the Casson hybrid nanofluid flow through a stretching surface with thermal radiation: a biomedical application. *The European Physical Journal Plus, 140*(2), 128.

[30] Najafi, N., Almosawy, W., Abbas, M. S., Goligerdian, A., Najafi, M., Abdi, N., ... & Aminian, S. (2025). Comparative analysis of the silver-gold and copper-titanium dioxide hybrid nanoparticles impact on flow and heat transfer of the pulsatile blood in occluded cerebral artery. *Journal of Thermal Biology, 127*, 104060.

[31] Hafed, Z. S., Arafa, A. A., Hussein, S. A., Ahmed, S. E., & Morsy, Z. (2025). Bioconvective blood flow of tetra composition nanofluids passing through a stenotic artery with Arrhenius energy. *Numerical Heat Transfer, Part B: Fundamentals, 86*(3), 580-603.

[32] Muhammad, T., Waqas, H., Manzoor, U., Farooq, U., & Rizvi, Z. F. (2022). On doubly stratified bioconvective transport of Jeffrey nanofluid with gyrotactic motile microorganisms. *Alexandria Engineering Journal, 61*(2), 1571-1583.

[33] Khan, S. A., Hayat, T., & Alsaedi, A. (2023). Bioconvection entropy optimized flow of Reiner-Rivlin nanoliquid with motile microorganisms. *Alexandria Engineering Journal, 79*, 81-92.

[34] Waqas, H., Farooq, U., Muhammad, T., Hussain, S., & Khan, I. (2021). Thermal effect on bioconvection flow of Sutterby nanofluid between two rotating disks with motile microorganisms. *Case Studies in Thermal Engineering, 26*, 101136.

[35] Nisar, Z., & Yasmin, H. (2023). Analysis of motile gyrotactic micro-organisms for the bioconvection peristaltic flow of Carreau–Yasuda bionanomaterials. *Coatings, 13*(2), 314.